J. of Korean Inst. of Resources Recycling
Vol. 18, No. 4, 2009, 24-30

≫ 研究論文 ≪

酸化티탄 나노粒子가 擔持된 칼슘 알루미늄 螢光體†

Dilip R. Thube*,** · **金鎭煥*** · **姜錫旻*** · **†柳鎬鎭***

韓國化學硏究院 에너지素材硏究센터

Calcium Aluminate Phosphor Supported TiO_2 Nanoparticles†

Dilip R. Thube*,, Jinhwan Kim*, Suk-min Kang* and †Hojin Ryu***

**Energy Materials Research Centre, Korea Research Institute of Chemical Technology,0 P.O. Box 107, Yuseong, Daejeon, 305-600, South Korea*

***Post-Graduate Department of Chemistry, New Arts, Commerce and Science College, Parner, Ahmednagar, 414 302 (MS), India*

요 약

희토류 원소를 기반으로한 알루미늄산 형광체에 담지된 산화티탄은 졸겔방법 으로 제조되었다. 이렇게 제조된 산화티탄 나노입자의 재료물성을 분석하기 위해 XRD, FT-IR, DRS UV-Vis, TEM 측정을 실시하였다. 형광체에 담지된 산화티탄 입자의 소결 전후의 XRD분석결과는 600도 이상의 온도에서 아나타제에서 루틸로 상변화가 일어나지 않았다. 600도 이상의 온도에서 지속적인(장시간) 열처리 후에도 형광체에 담지된 산화티탄이 결정화도가 높은 아나타제로 존재 하는 것은 형광체 지지체와 담지된 산화티탄의 서로 다른 결정입계에 의하여 결정성장과 상변화에 필요한 치밀화가 억제되기 때문으로 판단된다. DRS측정결과 형광체에 담지된 산화티탄은 산화티탄이 없는 형광체에 비하여 보다 긴 장파로 쉬프트한 것은 밴드갭 에너지의 환원을 나타낸다. 이러한 형광체에 담지된 산화티탄의 FT-IR 스펙트럼은 피크의 위치가 더 높은 파수로 이동하였다. 이것은 산화티탄 입자와 지지체 사이의 공유결합이 관계하기 때문 이라 판단된다. TEM 이미지는 형광체 지지체에 다른 입자 크기로 담지되어 있는 산화티탄의 분산, 결정화 및 입자 형상을 나타낸다.

주제어 : 희토류, 졸겔방법, 산화티탄, 아나타제, 열처리

Abstract

Rare earth based calcium aluminate phosphor ($CaAl_2O_4:Eu^{2+}$, Nd^{3+}) supported TiO_2 nanoparticles are synthesized by using sol-gel method, which are further characterized using powder X-ray diffraction (XRD), fourier transform infrared (FT-IR), diffuse reflectance UV-Visible spectroscopy (DRS UV-Vis) and transmission electron microscopy (TEM). The XRD pattern of as-prepared and sintered phosphor supported TiO_2 does not show the tendency to change the crystal structure from anatase to rutile phase up to 600°C. This indicates that the phosphor support might inhibit the densification and crystallite growth by providing dissimilar boundaries. The diffuse reflectance spectral (DRS) measurements showed shift towards longer wavelength indicating reduction in the band-gap energy as compared to free TiO_2. The FT-IR spectra of phosphor supported TiO_2 nanoparticles show shift in the peak positions to lower wavelengths. This indicates that the TiO_2 nanoparticles are not free, but covalently bonded to the phosphor support. TEM micrographs show presence of crystalline and spherical TiO_2 nanoparticles (8 - 15 nm diameter) dispersed uniformly on the surface of phosphor.

Key words : Sol-gel method, phosphor supported TiO_2, calcium aluminate, visible light photocatalyst, thermally stable anatase

†2009년 3월 3일 접수, 2009년 4월 24일 1차수정, 2009년 6월 12일 2차수정, 2009년 6월 17일 수리
†E-mail: hjryu@krict.re.kr

1. INTRODUCTION

In recent years, titania has been the material of

choice for its envisaged potential applications in energy and environmental sciences.[1] For example, TiO_2 has been utilized as a photocatalyst for photochemical hydrogen production and for self cleaning of windows. In the cosmetic industry, titania is the main ingredient in many commercial sunscreens and a strong competitor to ZnO on account of its UV absorption properties. The photocatalytic degradation is a promising technology for the removal of toxic organic and inorganic contaminants from water and waste water.[2-5] Among various photocatalysts, titania has been in the center stage of attraction mostly due to its high photocatalytic activity, strong oxidizing power, resistance to corrosion, photostability, chemical inertness, low cost and non-toxicity.[6-7] However, its applications were limited because of its large band-gap (3.20 eV for anatase TiO_2 phase), abosprtion in UV region (activated only by UV light) and the fact that the solar light has only a small fraction (8 %) of UV light as compared to visible light (45%).[8] Hence to make it efficient, manipulating the composition has become crucial for increasing its absorption range enabling efficient trapping of solar light. Many attempts, such as transition metal ion deposition,[9] anion doping[10-22] have been made to sensitize TiO_2 for improved absorption in the visible region. However doped materials suffer from thermal instability and increased carrier-recombination centers.[23] Several reports on the modification of TiO_2 nanoparticles with transition metal oxides and other oxides such as SiO_2, SnO_2, In_2O_3, (Sr, La)$TiO_{3+\delta}$ and $SrTiO_3$[24-27] exist which have been used to enhance the visible light absorption, however, the effect of alkaline earth metal aluminate phosphor support has not yet been investigated. Zheng *et al.* have reported that the light-storing phosphor and TiO_2 are combined together by coating forms light-storing photocatalyst.[32] This light storing photocatalyst can store light irradiation and emit slowly, as a result photocatalyst remains active when the light source is cut off. Existing bulk semiconducting materials possesses low surface area, less absorption property and fast electron-hole recombinations. In order to overcome these difficulties, research has been oriented towards the synthesis of nanomaterials for environmental applications.[28] Nanocrystalline materials exhibit unique properties such as quantum size effect, high surface area, short interface migration distance and visible light activity, all of which achieve enhanced photocatalytic performance. When particle size is smaller the number of active surface sites increases and thus does the surface charge carrier transfer rate in photocatalysis.[29-30] The sol-gel process is the novel technique for the preparation of nanocrystalline TiO_2 through which the physico-chemical and electrochemical properties of TiO_2 can be modified to improve its efficiency[1, 30-31]. Thus, in the present report, we attempted to modify the properties of TiO_2 by supporting it with optically sensitive phosphor materials. We have synthesized the phosphor supported TiO_2 nanoparticles by sol-gel method and characterized using X-ray diffraction (XRD), fourier transform infrared (FT-IR), diffuse reflectance UV-Visible spectroscopy (DRS UV-Vis) and transmission electron microscopy (TEM).

2. EXPERIMENTS

TiO_2 nanoparticles were synthesized using sol-gel method reported in the literature.[31] The nanoparticles obtained were heat treated at different temperatures from 300 to 600°C with a heating rate of 2°C min^{-1}. The phosphor supported TiO_2 nanoparticles were synthesized using sol-gel procedure as follows: A phosphor, calcium aluminate ($CaAl_2O_4:Eu^{2+},Nd^{3+}$, 1.2 g) was dispersed to a solution containing ethanol (115 g, Merck, 99.7%), deionized water (3.5 g) and a catalytic quantity of glacial acetic acid (0.035 g) with constant stirring for 30 min. To the above solution titanium (iv) isopropoxide (TIP), $Ti(OC_3H_7)_4$ (Aldrich, 97%), 0.24 M was added drop-wise over a period of approximately 10 min, under constant stirring. A white precipitate of TiO_2 immediately formed was stirred at 50°C for 5 min. This TiO_2 precipitate was dried in oven at 70-80°C for 48 h. The product obtained was calcined at 400°C and 600°C and characterized using XRD, FT-IR, DRS UV-Vis and TEM techniques. Schematic flow chart of sol-gel process used in this study is shown in Fig. 1.

The XRD patterns were recorded on a RIGAKU D/MAX 2200V, Japan X-ray diffractometer (Cu Kα radiation (λ=1.54059 Å), 40 kV and 40 mA). The diffractograms were recorded in the 2θ range 10-80° in steps of 0.02° s^{-1}. The crystallite size was estimated using the Scherrer equation,[33]

$$Dc = \frac{K\lambda}{B\cos\theta} \qquad \text{equation (1)}$$

where Dc is the average crystallite size; K (=0.89) is the Scherrer constant; λ (=1.54059 Å) is the X-ray wavelength; B is the full-width at half-maximum (FWHM) and θ is the diffraction angle. The identification of the different crystalline phases was accomplished using the JCPDS database.

FT-IR spectra were recorded with a BRUKER EQUINOX55 FT-IR spectrometer in the range of 4000–200 cm^{-1} on powders dispersed in KBR pellets. DRS UV-visible spectra were recorded using UV-vis spectrophotometer (Shimadzu 2401 PC), with $BaSO_4$ as a reference. The spectra were recorded at room temperature in air, in the range of 250 to 800 nm. TEM images of the materials were recorded with FEI TECNAI G^2 T-20S microscope. The surface morphologies and particle size was observed by TEM and high-resolution HRTEM, with an accelerating voltage of 200 kV.

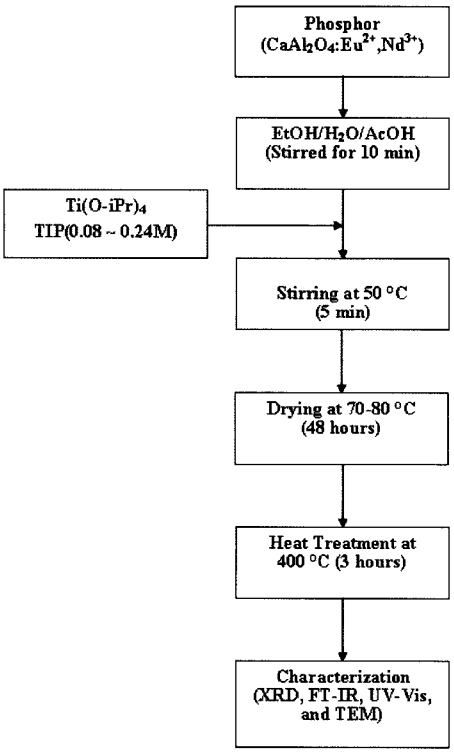

Fig. 1. Schematic flow chart of sol-gel process used for synthesis of phosphor supported TiO_2 nanoparticles.

3. RESULTS AND DISCUSSION

The crystal structure of a photocatalyst is an important property for the catalytic activity of the nanoparticles. The crystal structure of the synthesized free and the phosphor supported TiO_2 nanoparticles were studied by XRD. The characteristic XRD patterns for the free and phosphor supported TiO_2 nanoparticles sintered at various temperatures from 300 to 600°C in air are given in Fig. 2 (a) and (b) respectively. The XRD patterns for free TiO_2 nanoparticles sintered at 400°C in air correspond to the anatase TiO_2 while above 450°C corresponds to the both, anatase and rutile phase. Thus, the powder XRD pattern of as-prepared and sintered TiO_2 show the tendency to change the crystal structure from anatase to rutile with

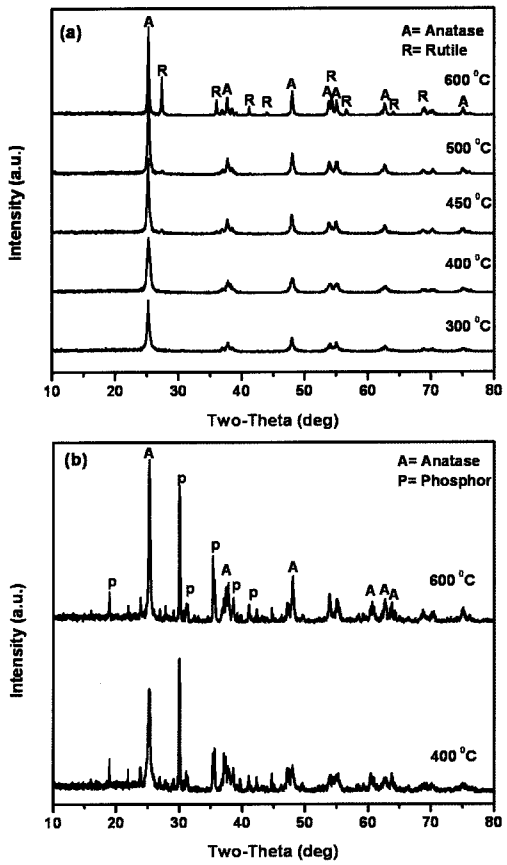

Fig. 2. XRD patterns of (a) free and (b) phosphor supported TiO_2 nanoparticles obtained at different calcination temperatures.

Table 1. Average crystallite sizes (nm) of free and phosphor supported TiO_2[a] at different calcination temperatures using XRD

Material	300°C, 3 h	400°C, 3 h	500°C, 3 h	600°C, 3 h
Free TiO_2	A: 20.48	A: 15.93	A: 22.12 R: 27.61	A: 32.91 R: 37.16
Phosphor Supported TiO_2	---	A: 16.91	---	A: 25.57

The average crystallite size of materials was determined by XRD using Scherrer equation.
[a]A and R denote anatase and rutile, respectively.

the temperature. The XRD patterns of phosphor supported TiO_2 nanoparticles sintered at 400 to 600°C correspond to the anatase TiO_2 phase only. This clearly indicates that the anatase phase of the phosphor supported TiO_2 nanoparticles is thermally stable till 600°C. This also implies that the modification by phosphor could retard the phase transformation of anatase to rutile and may lead to increase the surface area significantly.[22] The average crystalline sizes calculated from the (1 0 1) XRD peak of anatase and the (1 1 0) XRD peak of rutile are shown in Table 1. It can be noticed that the average crystalline size of the anatase phase in free TiO_2 increases with temperature indicating sintering of TiO_2 at high temperature. However, the data in Table 1 for phosphor supported TiO_2 indicates that the phase transformation is largely prevented due to support as reported earlier.[34-35] It is also observed that there is shift in the 2θ values of (1 0 1) diffraction peaks towards higher values. This may be a result of the formation of tetrahedral Ti species, whose interaction with the octahedral Ti sites in anatase is thought to prevent the phase transformation to rutile.[35-36] Further, the phosphor supported TiO_2 nanoparticles shows decrease in the intensity of the (1 0 1) XRD peak of anatase as compared to the free TiO_2 which may be due to the chemical interactions between the surfaces of the phosphor and TiO_2 particles. The results of the XRD study are well supported by TEM studies of the synthesized materials.

FT-IR spectra for free and phosphor supported TiO_2 nanoparticles are given in Fig. 3. The characteristic Ti-O-Ti absorptions are found in the range of 500-1000 cm^{-1}. The broad absorption peak of pure TiO_2 assigned to the Ti-O-Ti bond appears at 543 cm^{-1},[38-40] whereas for phosphor supported TiO_2 it appears at 634 cm^{-1}. The FT-IR spectra of phosphor supported TiO_2 nanoparticles show the increase in the wavenumbers of the characteristic vibrations of TiO_2 as compared with

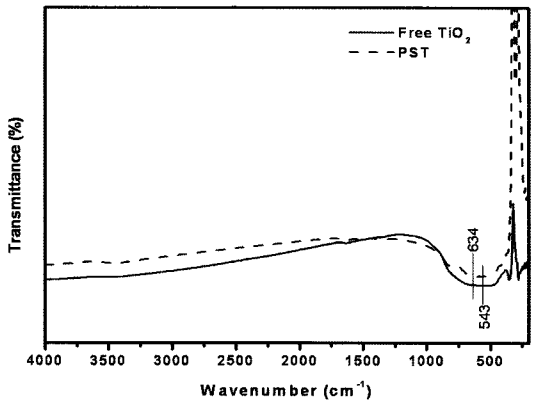

Fig. 3. FT-IR spectra of free and phosphor supported TiO_2 nanoparticles (PST - phosphor supported TiO_2).

free TiO_2. This may be partly attributed to the transfer of electronic cloud from the terminal oxidic sites would result the suppression of back donation of the same to the titanium sites through antibonding molecular orbitals which may lead to the strengthening of Ti-O sigma (ó) bonds in the entire nano-TiO_2 particles. Thus, it could be said that the TiO_2 nanoparticles are not free but covalently bound to the phosphor support.

To investigate the absorption band shifts of TiO_2, DRS were recorded and analyzed. DRS UV-vis reflectance spectra of the free and phosphor supported TiO_2 nanoparticles are shown in Fig. 4. The absorbance maximum for free TiO_2 is 396 nm, whereas for phosphor supported TiO_2 it is at 405 nm. Generally, the shift of the absorption band towards the longer wavelength region with the increase in the crystallite sizes of the materials indicates the decrease in the band-gap energy due to the quantum size effects.[41-44] The as-synthesized phosphor supported TiO_2 nanoparticles shows shift in the absorption band toward the longer wavelength region, which indicates the decrease in the

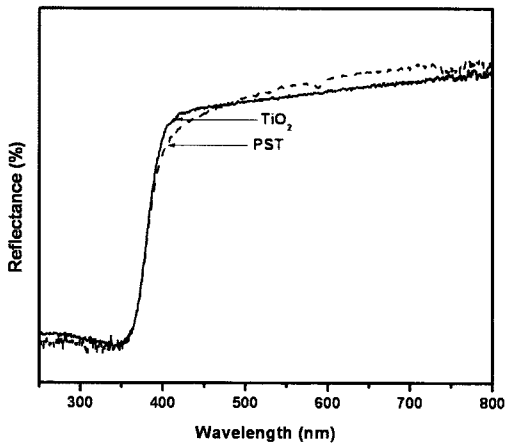

Fig. 4. UV-Visible diffuse reflectance spectra for free and phosphor supported TiO_2 nanoparticles (PST - phosphor supported TiO_2).

band-gap energy. This decrease in band-gap energy may be due to the covalent interactions between the surface of phosphor and TiO_2 nanoparticles.

TEM study is an appropriate tool to understand the structural and morphological transformations of the material. The morphology of synthesized nanoparticles is studied using TEM and high-resolution HRTEM images and selected area electron diffraction (SAED) patterns. Fig. 5 (a) and (b) shows the TEM micrographs and corresponding SAED patterns for the free and phosphor supported TiO_2 nanoparticles respectively. A TEM image of phosphor supported TiO_2 nanoparticles clearly reveals the crystalline and spherical nature of the nanoparticles with the average grain size of 8-15 nm. It is also observed that the average crystalline size of phosphor supported TiO_2 nanoparticles is smaller as compared to free TiO_2 with TiO_2 nanoparticles uniformly dispersed on the surface of phosphor material. Occasional aggregation of TiO_2 nanoparticles is also observed. The morphology of the as-prepared TiO_2 nanoparticles remains same while the particle size is decreased to 8 - 15 nm. The covalent interactions between TiO_2 nanoparticles and support might be the reason for observed uniform dispersion. Such a size controlling donor-acceptor mechanism is greatly evidenced in this study. Although TiO_2 particles are of nanosize, they appear to have the different sizes. It is attributed to the difference in the Lewis acid strength of different sites on the surface of phosphor material.

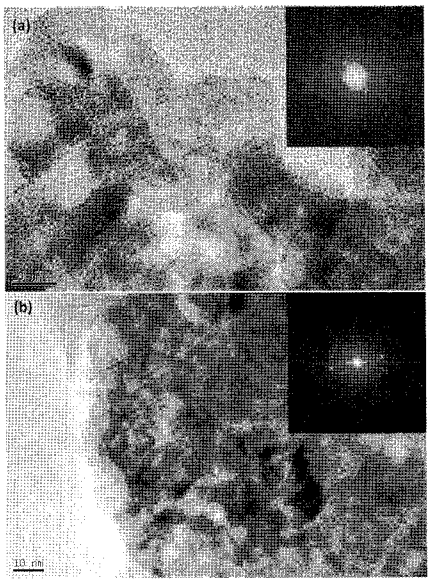

Fig. 5. TEM micrographs for (a) free and (b) phosphor supported TiO_2 nanoparticles (Inset shows corresponding SAED pattern).

4. CONCLUSIONS

The phosphor supported TiO_2 nanoparticles were successfully synthesized by sol-gel method. The particle size of as-prepared phosphor supported TiO_2 nanoparticles is found to be smaller (8-15 nm) than free TiO_2 (~25 nm). The smaller particle size is known to improve the surface area which is important in catalysis. Phosphor supported TiO_2 nanoparticles exhibit excellent thermal stability which retards the anatase to rutile phase transition in TiO_2 has been confirmed from XRD data. The as-prepared TiO_2 nanoparticles show covalent interactions with the phosphor support and hence, show absorption towards the longer wavelength in the diffuse reflectance spectra. Thus, the band-gap of these photocatalysts can be tuned to improve the absorption in the visible spectrum of solar light and further work in this direction is underway.

ACKNOWLEDGEMENT

Author D. R. Thube is grateful to Korea Federation of Science & Technology KOFST, South Korea, for the fellowship under Brain Pool Program.

REFERENCES

1. X. Chen, and S. S. Mao, 2007: Titanium Dioxide Nanomaterials: Synthesis, Properties, Modifications, and Applications, Chem. Rev. **107**, pp. 2891-2959.
2. D. F. Ollis, and C. S. Turchi, 1990: Heterogeneous photocatalysis for water purification: Contaminant mineralization kinetics and elementary reactor analysis, Environ. Prog. **9**, pp. 229-234.
3. D. W. Bahnemann, E. Pelizzetti, and M. Schiavello (Eds.), 1991: Photochemical Conversion and Storage of Solar Energy, Kluwer Academic Publishers, Dordrecht, The Netherlands, pp. 251-276.
4. M. R. Hoffmann, S. T. Martin, W. Choi, and D. W. Bahnemann, 1995: Environmental Applications of Semiconductor Photocatalysis, Chem. Rev. **95**, pp. 69-96.
5. A. Mills, and S. L. Hunte, 1997: An Overview of Semiconductor Photocatalysis, J. Photochem. Photobiol. **A 108**, pp. 1-35.
6. M. A. Fox, and M. T. Dulay, 1993: Heterogenous Photocatalysis, Chem. Rev. **93**, pp. 341-357.
7. M. V. Shankar, S. Anandan, N. Venkatachalam, B. Arbindoo, and V. Murugesan, 2004: Novel thin-film reactor for photocatalytic degradation of pesticides in an aqueous solution, J. Chem. Technol. Biotechnol. **79**, pp. 1279-1285.
8. T. L. Thompson, and J. T. Yates-Jr, 2006: Surface Science Studies of the Photoactivation of TiO_2 New Photochemical Process, Chem. Rev. **106**, pp. 4428-4453.
9. S. Sakthivel, and H. Kisch, 2003: Daylight Photocatalysis by Carbon-Modified Titanium Dioxide, Angew. Chem. Int. Ed., **42**, pp. 4908-4911.
10. H. Irie, Y. Watanabe, and K. Hashimoto, 2003: Carbon-doped Anatase TiO_2 Powders as a Visible-light Sensitive Photocatalyst, Chem. Lett. **32**, pp. 772-774.
11. T. Umebayashi, T. Yamaki, S. Tanaka, and K. Asai, 2003: Visible Light-Induced Degradation of Methylene Blue on S-doped TiO_2, Chem. Lett., **32**, pp. 330-332.
12. T. Ohno, T. Mitsui, and M. Matsumura, 2003: Visible Light-Induced Degradation of Methylene Blue on S-doped TiO_2, Chem. Lett., **32**, pp. 364-365.
13. J. C. Yu, J. G. Yu, W. K. Ho, Z. T. Jiang, and L. Z. Zhang, 2002: Effects of F^- Doping on the Photocatalytic Activity and Microstructures of Nanocrystalline TiO_2 Powders, Chem. Mater., **14**, pp. 3808-3816.
14. T. Lindgren, J. M. Mwabora, E. Avendano, J. Jonsson, A. Hoel, C.-G. Granqvist, and S.-E. Lindquist, 2003: Photoelectrochemical and Optical Properties of Nitrogen Doped Titanium Dioxide Films Prepared by Reactive DC Magnetron Sputtering, J. Phys. Chem. B, **107**, pp. 5709-5716.
15. T. Ihara, M. Miyoshi, Y. Iriyama, O. Matsumoto, and S. Sugihara, 2003: Visible-light-active titanium oxide photocatalyst realized by an oxygen-deficient structure and by nitrogen doping, Appl. Catal. B, **42**, pp. 403-409.
16. C. Lettmann, K. Hildenbrand, H. Kisch, W. Macyk, and W. F. Maier, 2001: Visible light photodegradation of 4-chlorophenol with a coke-containing titanium dioxide photocatalyst, Appl. Catal. B, **32**, pp. 215-227.
17. W. Zhao, W. Ma, C. Chen, J. Zhao, and Z. Shuai, 2004: Efficient Degradation of Toxic Organic Pollutants with $Ni_2O_3/TiO_{2-x}B_x$ under Visible Irradiation, J. Am. Chem. Soc., **126**, pp. 4782-4783.
18. H. Irie, S.Washizuka, N. Yoshino, and K. Hashimoto, 2003: Visible-light induced hydrophilicity on nitrogen-substituted titanium dioxide films, Chem. Commun., pp. 1298-1299.
19. H. Irie, Y. Watanabe, and K. Hashimoto, 2003: Nitrogen-Concentration Dependence on Photocatalytic Activity of $TiO_{2-x}N_x$ Powders, J. Phys. Chem. B, **107**, pp. 5483-5486.
20. J.L. Gole, J.D. Stout, C. Burda, Y. Lou, and X. Chen, 2004: Highly Efficient Formation of Visible Light Tunable $TiO_{2-x}N_x$ Photocatalysts and Their Transformation at the Nanoscale, J. Phys. Chem. B, **108**, pp. 1230-1240.
21. L. Lin, W. Lin, Y. X. Zhu, B. Y. Zhao, and Y. C. Xie, 2005: Phosphor-doped Titania -a Novel Photocatalyst Active in Visible Light, Chem. Lett., **34**, pp. 284-285.
22. L. Lin, R. Y. Zheng, J. L. Xie, Y. X. Jhu, and Y. C. Xie, 2007: Synthesis and characterization of phosphor and nitrogen co-doped titania, App. Catal. B: Environ., **76**, pp. 196-202.
23. A. Asahi, T. Morikawa, T. Ohwaki, K. Aoki, and Y. Taga, 2001: Visible-Light Photocatalysis in Nitrogen-Doped Titanium Oxides, Science, **293**, pp. 269-271.
24. D. Shchukin, S. Poznyak, A. Kulak, and P. Pichat, 2004: TiO_2-In_2O_3 photocatalysts: preparation, characterizations and activity for 2-chlorophenol degradation in water, J. Photochem. Photobiol. A: Chem., **162**, pp. 423-430.
25. S. Otsuka-Yao- Matsuo, and M. Ueda, 2004: Visible light-induced photobleaching of methylene blue aqueous solution using $(Sr_{1x}La_x)TiO_{3+ä}$–TiO_2 composite powder, J. Photochem. Photobiol. A: Chem., **168**, pp. 1-6.
26. P. Cheng, W. Li, T. Zhou, Y. Jin, and M. Gu, 2004: Physical and photocatalytic properties of zinc ferrite doped titania under visible light irradiation, J. Photochem. Photobiol. A: Chem., **168**, pp. 97-101.
27. F. X. Ye, T. Tsumura, K. Nakata, and A. Ohmoric, 2008: Dependence of photocatalytic activity on the compositions and photo-absorption of functional TiO_2–Fe_3O_4 coatings deposited by plasma spray, Mater. Sci. Eng. B, **148**, pp. 154-161.
28. H. Wang, Y. Wu, and B. Q Xu, 2005: Preparation and characterization of nanosized anatase TiO_2 cuboids for photocatalysis, Appl. Catal. B Environ., **59**, pp. 139-146.
29. R. S. Sonawane, B. B. Kale, and M. K. Dongare, 2004: Preparation and photo-catalytic activity of Fe–TiO_2 thin films prepared by sol-gel dip coating, Mater. Chem. Phys., **85**, pp. 52-57.
30. N. Venkatchalam, M. palanichamy, and V. Murugesan, 2007: Sol-gel preparation and characterization of nanosize TiO_2: Its photocatalytic performance, Mater. Chem. Phys., **104**, pp. 454-459.
31. J. N. Hart, L. Bourgeosis, R. Cervini, Y. B. Cheng, G. P.

Simon, and L. Spiccia, 2007: Low temperature crystallization behavior of TiO_2 derived from a sol–gel process, J Sol-Gel Sci. Tech., **42**, pp. 107-117.
32. J. Zhang, F. Pan, W. Hao, Qi Ge, and T. Wang, 2004: Light-storing photocatalyst, Appl. Phys. Letts., **85**, pp. 5778-5781.
33. B. D. Cullity (Ed.), 1978: Elements of X-Ray Diffraction, 3rd Edn. Addision-Wesley, Reading, MA, pp. 102, 284.
34. A. K. Datye, G. Riegel, J. R. Bolton, M. Haung, and M. R. Prairie, 1995: Microstructural Characterization of a Fumed Titanium Dioxide Photocatalyst, J. Solid State Chem., **115**, pp. 236-239.
35. Y. H. Zhang, H. X. Zhang, Y. X. Xu, and Y. G. Wang, 2004: Significant effect of lanthanide doping on the texture and properties of nanocrystalline mesoporous TiO_2, J. Solid State Chem., **177**, pp. 3490-3498.
36. S. Hishita, I. Mutoh, K. Koumoto, and H. Yanagida, 1983: Inhibition mechanism of the anatase-rutile phase transformation by rare earth oxides, Ceram. International, **9**, pp. 61-67.
37. J. Nair, P. Nair, F. Mizukami, Y. Oosawa, and T. Okuba, 1999: Microstructure and phase transformation behavior of doped nanostructured titania, Mater. Res. Bull., **34**, pp. 1275-1290.
38. N. Venkatchalam, M. Palanichamy, and V. Murugesan, 2007: Sol–gel preparation and characterization of alkaline earth metal doped nano TiO_2: Efficient photocatalytic degradation of 4-chlorophenol, J. Mol. Catal. A: Chem., **273**, pp. 177-185.
39. W. Bauer, and G. Tomandl, 1994: Preparation of spherical TiO_2 particles by an emulsion method using $TiCl_4$, Ceram. International, **20**, pp. 189-193.
40. M. Ocana, V. Fornes, and C. J. Sema, 1992: A simple procedure for the preparation of spherical oxide particles by hydrolysis of aerosols, Ceram. International, **18**, pp. 99-106.
41. Z. Li, B. Hou, Y. Xu, D. Wu, and Y. Sun, 2005: Hydrothermal synthesis, characterization, and photocatalytic performance of silica-modified titanium dioxide nanoparticles, J. Colloid. Interface. Sci., **288**, pp. 149-154.
42. Z. Wang, L. Mao, and J. Lin, 2006: Preparation of TiO_2 nanocrystallites by hydrolyzing with gaseous water and their photocatalytic activity, J. Photochem. Photobiol. A: Chem., **177**, pp. 261-268.
43. D. S. Kim, S. J. Han, and S. Y. Kwak, 2007: Synthesis and photocatalytic activity of mesoporous TiO_2 with the surface area, crystallite size, and pore size, J. Colloid. Interface. Sci., **316**, pp. 85-91.
44. M. Anpo, T. Shima, S. Kodama, and Y. Kubokawa, 1987: Photocatalytic hydrogenation of propyne with water on small-particle titania: size quantization effects and reaction intermediates, J. Phys. Chem., **91**, pp. 4305-4310.
45. S. Sivakumar, P. Krishna, P. Mukundan, and K. G. K. Warrier, 2002: Sol–gel synthesis of nanosized anatase from titanyl sulfate, Mater. Lett., **57**, pp. 330-335.

Dilip R. Thube

- Ph.D.: 2002, Chemistry, University of Pune, Pune, India.
- M.Sc.: 1993, Chemistry, University of Pune, Pune, India.
- B.Sc.: 1991, Chemistry, University of Pune, Pune, India.
- Position: Associate Professor, Post-Graduate Department of Chemistry, New Arts, Commerce and Science College, Parner, Dist-Ahmednagar, India.
- Presently: Brain Pool Scientist of KOFST at KRICT, Daejeon, Korea.

金 鎭 煥

- 1994.03-2003.02 (Bachelor, Master) Pukyong National University in Korea, Department of Material Science and Engineering
- 2004.04-2008.02 (Doctor, Post-doctor) Yokohama National University in Japan, Department of Material Science and Engineering
- 2008.9-2009.5 (Post-doctor) KRICT in Korea, Energy Materials Research Center
- 2009.05- now SBLimotive in Korea

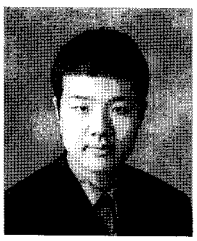

姜 錫 旻

- 2000.02-2009.02 (Bachelor, Master) Chungnam National University in Korea, Department of Chemistry
- 2009.3- now (Pre-doctor) KRICT in Korea, Energy Materials Research Center

柳 鎬 鎭

- 현재 한국화학연구원 에너지소재연구센터 책임연구원
- 당 학회지 제16권 5호 참조